The Q-band (43 GHz) Celestial Reference Frame Observed in 2021

Hana Krásná[1], Aletha de Witt[2], Christopher S. Jacobs[3], David Gordon[4], Frédéric Jaron[1], Taehyun Jung[5]

Abstract Our Q-band (43 GHz) celestial reference frame, based on three dual-polarization VLBA sessions from 2021, has 428 sources and 67 thousand observations. The primary goal of these sessions was to compare the structure of the active galactic nuclei (AGN) observed at Q-band (43 GHz) to S, X, and K-bands (2.3, 8.4, and 24 GHz) using nearly concurrent VLBA sessions. The solution presented here was made with the VieVS software on February 09, 2024. Median formal precisions are 203 µas in $\alpha \cos\delta$ and 353 µas in δ. This Q-band frame is based solely on the all northern geometry of the VLBA. As a result, sky coverage is limited to declinations above -45 deg and precision tends to decrease as one moves south. We are exploring the potential to add Q-band VLBI observations using the Korean tri-band (K, Q, W-band) system. In the far south, we are exploring the baseline from Mopra, Australia to the CART 40-m antenna in Argentina. The prospects for future improvements are bright with the aforementioned potential for adding new stations as well as plans for proposing for more Q-band time on the VLBA, and the planned VLBA upgrade from 4 to 8 Gbps data rates.

Keywords VLBA, Q-band, CRF

1. Technische Universität Wien (TU Wien), Austria
2. South African Radio Astronomy Observatory (SARAO), South Africa
3. Jet Propulsion Laboratory, California Institute of Technology (JPL), USA
4. U.S. Naval Observatory (USNO), USA
5. Korea Astronomy and Space Science Institute (KASI), South Korea

1 Introduction

Celestial reference frames from VLBI are based on observations of radio signals from active galactic nuclei (AGN). Nowadays, VLBI telescopes typically observe signals across multiple radio bands. This also reflects the ICRF3 (Charlot et al. 2020 [2]), the currently adopted CRF by the International Astronomical Union (IAU), which includes radio source positions at X-band (8.4 GHz), K-band (24 GHz), and Ka-band (32 GHz). In this work we analyzed 67 thousand observations based on three Very Long Baseline Array (VLBA; Napier 1995 [9]) dual-polarization sessions from 2021 whose primary goal was to compare the structure of active galactic nuclei (AGN) observed at Q-band (43 GHz) to S, X, and K-bands (2.3, 8.4, and 24 GHz) using nearly concurrent VLBA sessions. Previous work at Q-band was done by Lanyi et al. (2010) [6] with the VLBA and Petrov et al. (2012) [10] with the Korean VLBI Network.

On VLBI scales, as radio frequencies increase, the AGN tend to be more core dominated as the extended structure in the jets tends to fade away with increasing frequency (Figures 1 and 2). The spatial offset of the emissions from the AGN engine due to opacity effects (“core shift”) is reduced as frequency increases. Near-simultaneous S (2.3 GHz), X (8.4 GHz), K (24 GHz), and Q-band (43 GHz) images based on VLBA observations of 453 ICRF sources between April – June 2021 (Hunt et al., 2022 [4]; de Witt et al., 2022 [1]) demonstrate that these reference frame sources get more compact with increasing frequency (Figure 1). In particular, note how the jet fades with increasing frequency. The example shown is of source NRAO 140 (J0336+3218).

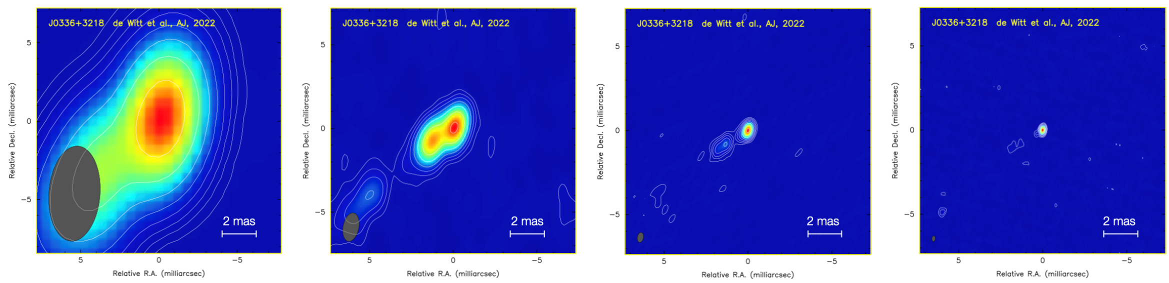

Fig. 1 Near-simultaneous S (2.3 GHz), X (8.4 GHz), K (24 GHz), and Q-band (43 GHz) images based on VLBA observations of NRAO 140 (J0336+3218). The VLBA synthesized beam is shown as the grey ellipse in each sub-figure (de Witt et al., 2022 [1]).

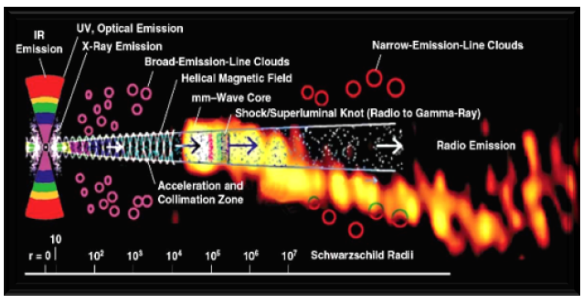

Fig. 2 Schematic of Active Galactic Nuclei (Marscher, 2006 [7]; Krichbaum et al., 1999 [5]; Wehrle et al., 2010 [11]).

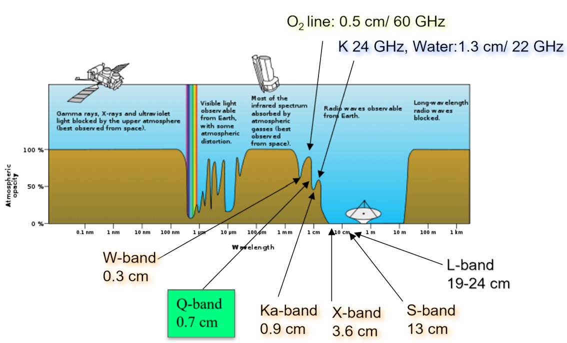

Fig. 3 The radio "window" is transparent compared to most of the spectrum. Q-band (43 GHz): above the 22 GHz H20 line, below the 60 GHz O2 line, is partially transparent. (credit: NASA)

We summarize the advantages and disadvantages of VLBI observations at Q-band to the lower radio frequencies as follows:

Advantages of Q-band compared to S/X-band:

- More compact, stable sources (Figsures 1 and 2)
- Reduced opacity effects: "core shift"
- Ionosphere reduced by nine times vs. S/X and by three times vs. K-band

Disadvantages of Q-band:

- More weather sensitive (Figure 3)
- Shorter coherence times
- Weaker sources, many resolved
- Antenna pointing is more difficult
- Combined effect is lower sensitivity

The disadvantages of the Q-band are rapidly being compensated by increasing data rates. The VLBA currently operates at 4 Gbps and has plans to upgrade to 8 Gbps.

2 Data

The data collected has been observed with the Very Long Baseline Array (VLBA) which consists of ten 25-meter telescopes forming 45 baselines with the longest East-West baseline being over 8,000 km. The longest North-South baseline is about 3,000 km leading to significantly lower declination precision. When the CART 40-m antenna comes online in Argentina, it has potential for a baseline to Mopra, Australia to complete coverage in the far south. Figure 4 shows the global distribution of existing and potential future antennas with Q-band receivers. We group these antennas in four groups:

1. with legacy Q-band receivers (blue),
2. with dual- or tri-band Korean-type receivers (K/Q/W) (red),
3. in the process of installing a Korean-type receiver (green), and
4. that indicated that they plan to install a Korean-type receiver (orange).

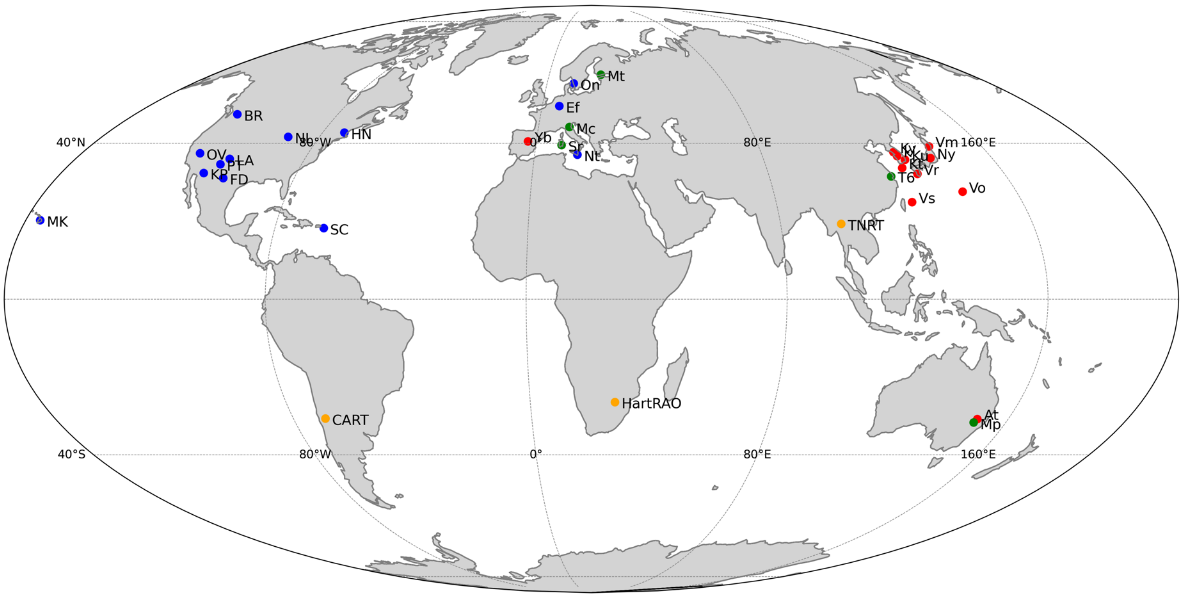

Fig. 4 Q-band antenna network: existing and potential future sites.

3 Results

Comparing this Q-band CRF (solution 2024/02/09) to the ICRF3-SX (Charlot et al, 2020 [2]), after removing poorly observed sources (less than three observations) and five outliers (angular separation larger than 5-σ), there are 399 common sources. Weighted root mean square (wrms) agreement is 211 µas and 316 µas in right ascension ($\alpha \cos\delta$) and declination (δ), respectively. Vector Spherical Harmonics (VSH; Mignard and Klioner, 2012 [8]) largest differences are X-dipole = 89 ± 23 µas and quadrupole 2,0 magnetic term = -66 ± 16 µas. Note that the small number of sessions and lack of any southern stations required us in addition to the usual No-Net-Rotation constraint to artificially constrain the $\Delta\delta$ vs. δ slope to ICRF3-SX until North-South baseline data can be added to stabilize the Q solution vs. δ.

Figures 5–10 summarize the statistics obtained from the Q-band CRF catalog as follows:

- Figure 5. Number of sessions: median number of sessions is two (i.e., one with dual polarization).
- Figure 6. Number of delay observations: median = 137 (RCP and LCP delays counted separately).
- Figure 7. $\alpha \cos\delta$ (arc) precision: median σ is 203 µas for 428 sources. No coverage for $\delta < -45°$.
- Figure 8. δ precision: median σ is 353 µas for 428 sources. No coverage for $\delta < -45°$.
- Figure 9. Error ellipse axes ratio A_{major}/A_{minor} shows steady elongation from δ +90° to $-45°$.
- Figure 10. Direction of error ellipses: semi-major axes are mostly North-South, i.e., δ estimate is weaker than α.

3.1 Gaia Optical-Radio Frame Tie and Accuracy Verification

Gaia (Global Astrometric Interferometer for Astrophysics) is a European Space Agency astronomical observatory mission launched in December 2013. It measures positions, proper motions, and parallaxes of 1.8 billion objects down to the 21st magnitude—as well as photometric and radial velocity measurements. Gaia's observations include more than 1.6 million AGN of which about 20,000 are optically bright (V < 18 mag)[1].

The Gaia celestial frame is independent from Q-band in three key respects: optical vs. radio, space vs. ground, pixel centroiding vs. interferometry. As a result, Gaia provides the most independent check of ac-

[1] https://www.esa.int/Science_Exploration/Space_Science/Gaia

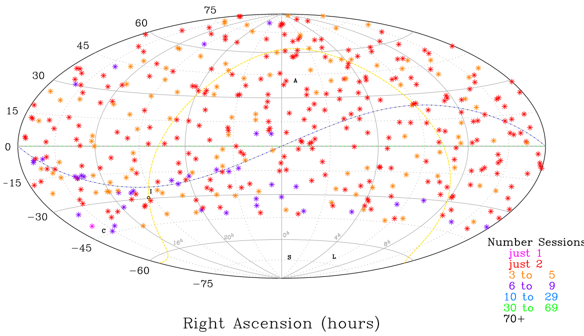

Fig. 5 Number of sessions.

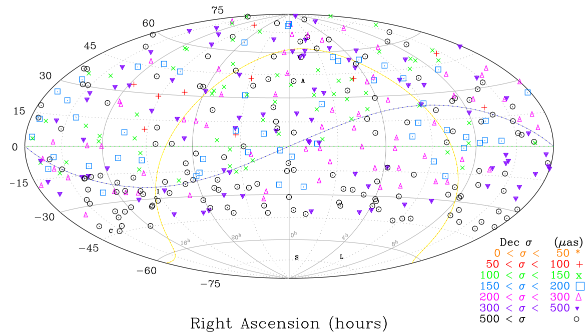

Fig. 8 δ precision.

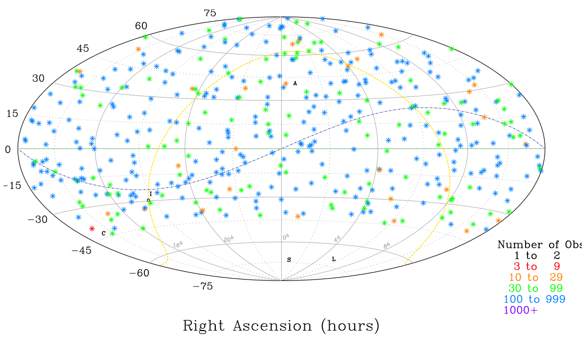

Fig. 6 Number of delay observations.

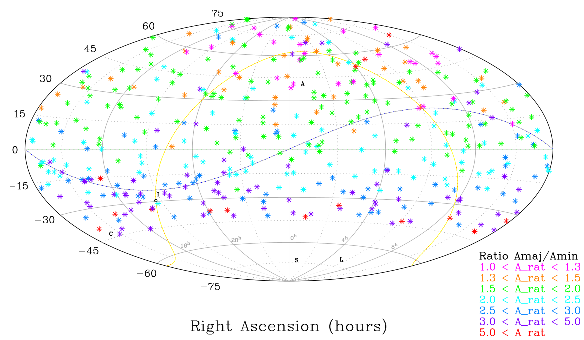

Fig. 9 Error ellipse axes ratio.

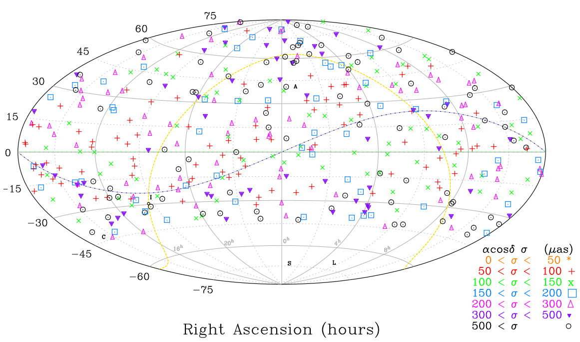

Fig. 7 $\alpha \cos \delta$ precision.

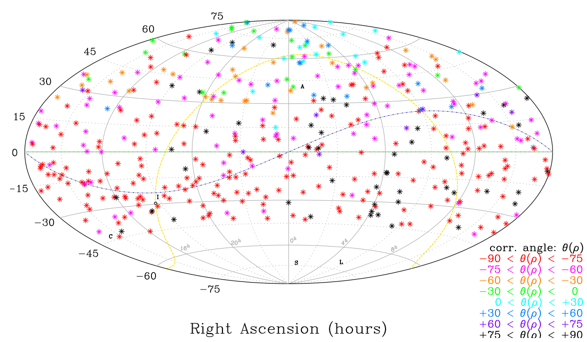

Fig. 10 Direction of error ellipses.

curacy available today. For our comparison we use the Gaia Early Data Release-3 (Gaia Collaboration, 2022 [3]). It includes 334 sources which are usable in both the optical and Q-band radio—after removing 23 outliers, where the angular separation between our Q-band solution and the Gaia position is larger than 5-σ ($\sim 6\%$ of the Q-band CRF).

The comparison results can be summarized in the following way:

- The rotational alignment is made with ~ 35 µas precision (1-σ, per 3-D component)
- The wrms scatter is 286 µas in $\alpha \cos \delta$ and 371 µas in δ
- Vector Spherical Harmonics (VSH) largest differences are X-dipole of 86 ± 31 µas, quadrupole 2,0 magnetic/electric -69 ± 24 µas / 78 ± 35 µas, and quadrupole 2,1 electric-imaginary of -75 ± 39 µas.

Overall, global agreement of the two frames is at the ~1.5 parts per billion level.

4 Conclusions

Our Q-band CRF has 428 AGN covering the sky with declination above $-45°$ and is poised for rapid improvements in precision. The median precision is 203 µas in $\alpha \cos \delta$ and 353 µas in δ. Spherical harmonic differences vs. ICRF3-SX are $\leq$ 90 µas and scatter vs. Gaia are $\leq$ 90 µas. Improving accuracy depends on controlling systematics via adding southern stations to the geometry.

Acknowledgements

We acknowledge use of the Very Long Baseline Array under the US Naval Observatory's time allocation. This work supports USNO's ongoing research into the celestial reference frame and geodesy.

The VLBA is operated by the National Radio Astronomy Observatory, which is a facility of the National Science Foundation operated under cooperative agreement by Associated Universities, Inc.

Part of this research was carried out at the Jet Propulsion Laboratory, California Institute of Technology, under a contract with the National Aeronautics and Space Administration (contract 80NM0018D0004, Copyright©2024, all rights reserved).

HK and FJ acknowledge the support by the Austrian Science Fund FWF – SOFT P 35920.

References

1. de Witt et al., Multi-Frequency Imaging Results of 452 Extragalactic ICRF-3 Radio Sources from Multi-Epoch, Near-Simultaneous Astrometric VLBA Observations. 15th EVN Symposium, Cork, Ireland, July 2022. https://www.ucc.ie/en/media/academic/physics/15thevn/2022/Aletha_deWitt.pdf
2. Charlot et al., ICRF3, A&A, 644, A159, 2020. https://doi.org/10.1051/0004-6361/202038368
3. Gaia Collaboration, Gaia-CRF3, A&A, 667, A148, 2022. https://doi.org/10.1051/0004-6361/202243483
4. Hunt et al., Comparing Images of ICRF Sources at S, X, K, and Q-band, IAU, FM7, 2022. https://doi.org/10.5281/zenodo.7068278
5. Krichbaum et al., High Angular Resolution Monitoring of Prominent AGN at 86 GHz, Proc. 2nd VLBI mm workshop, 1999. https://doi.org/10.48550/arXiv.astro-ph/9909176
6. Lanyi et al., The CRF at 24 and 43 GHz: I. Astrometry, AJ, 139, 5, 2010. https://doi.org/10.1088/0004-6256/139/5/1695
7. Marscher, Relativistic Jets in AGN, Proc. AIP, 856, 2006. https://doi.org/10.1063/1.2356381
8. Mignard and Klioner, Analysis of astrometric catalogues with vector spherical harmonics, A&A, 547, A59, 2012. https://doi.org/10.1051/0004-6361/201219927
9. Napier, Very Long Baseline Interferometry and the VLBA, ASP Conference Series, 82, 59–72, 1995. https://articles.adsabs.harvard.edu/pdf/1995ASPC...82...59N
10. Petrov, Early Science with KVN, QCAL1 43 GHz Calibrator Survey, AJ, 145, 5, 2012. https://doi.org/10.1088/0004-6256/144/5/150
11. Wehrle et al, Submillimeter, Near-Infrared and Optical Light Curves of Gamma-Ray Blazars, BAAS, 342, 375, 2010. https://ui.adsabs.harvard.edu/abs/2010AAS...21543405W/abstract